Chemical composition of volcanic glasses in visible tephra layers found in a 2503 m deep ice core from Dome Fuji, Antarctica

Mika KOHNO,[1] Yoshiyuki FUJII,[1] Takafumi HIRATA[2]

[1]*National Institute of Polar Research, Kaga, Itabashi-ku, Tokyo 173-8515, Japan*
E-mail: mkohno@pmg.nipr.ac.jp
[2]*Tokyo Institute of Technology, Ookayama 2-12-1, Meguro-ku, Tokyo 152-8551, Japan*

ABSTRACT. Twenty-six ash layers were found in a 2503 m deep ice core from Dome Fuji station, East Antarctica. In order to gain information about the sources of ash particles found in the layers, major and trace element abundances have been measured. The particles found in 21 of the 26 layers were commonly a few tens of μm in size, suggesting that they originated from volcanoes located in and around the Antarctic. On the basis of comparison of the major-element compositions of these tephras with reference to volcanic rocks and ash, the tephras were divided into three types: (1) tholeiitic basalt to dacite, (2) calc-alkaline andesite, and (3) trachyandesite to trachyte. The source regions appear to be (1) South Sandwich Islands, Southern Ocean, (2) South Shetland Islands, Antarctica, and/or a southern part of the volcanic zone of the Andes, and (3) Marie Byrd Land and/or Victoria Land, Antarctica, respectively. The tephras found in the other five ash layers were significantly smaller (< 5 μm), suggesting that they traveled over longer distances. Abundances of trace elements for the alkaline tephra collected from one layer revealed a possible genetic link to volcanic rocks from Marie Byrd Land. In order to correlate between ice cores from Dome Fuji and Vostok, Antarctica, which are widely separated, we found coeval ash layers serving as stratigraphic markers of Antarctic ice cores. A comparison of profiles of $^{18}O/^{16}O$ ($\delta^{18}O$) and $^{2}H/^{1}H$ (δD) for the Dome Fuji and Vostok cores indicates that eight ash layers are equivalent in the two cores. A clear correlation was found for the chemical compositions of six of these ash layers, indicating a high potential for key correlation beds between the deep ice cores from Dome Fuji and Vostok.

INTRODUCTION

Large amounts of volcanic ash and gases are emitted to the upper troposphere and stratosphere during explosive volcanic eruptions. The volcanic gases are converted into aerosols of sulfuric acid, and these acidic components mix with fine ash and are globally distributed. They eventually fall to the Earth's surface through complex physico-chemical processes. Ice cores drilled from the polar ice sheets can provide key information about the mechanism of global circulation of these volcanic products. They also provide a detailed record of local and distal volcanic eruptions as acidity peaks due to high concentrations of H_2SO_4, HCl and HF (e.g. Hammer and others, 1980) and/or as visible ash layers. The ash layers have been found in ice cores from Byrd (Gow and Williamson, 1971; Kyle and Jezek, 1978; Kyle and others, 1981; Palais, 1985), Dome C (Kyle and others, 1981) and Vostok (Kyle and others, 1984; Palais and others, 1987, 1989a, b, 1990; Basile and others, 2001) in Antarctica.

Chemical composition of the tephra in those cores has been used to estimate their source volcanic regions or, in some cases, source volcanoes (e.g. Cole-Dai and others, 1997). Genetic information on the tephras can play a role in (1) constructing the past history of explosive volcanic eruptions, (2) providing key beds for correlating not only Antarctic ice cores but also sea sediment cores around Antarctica, and possibly dating these cores, and (3) clarifying the relation between the past volcanism and climate change.

Twenty-six ash layers were found in a 2503 m deep ice core from Dome Fuji station (77°19′01″ S, 39°42′12″ E; 3810 m a.s.l.; Fujii and others, 1999; Fig. 1), which was obtained by the 36th to 37th Japanese Antarctic Research Expeditions in 1995 and 1996, located at the summit of the inland plateau in Dronning Maud Land, East Antarctica (Dome-F Deep Coring Group, 1998). In order to investigate the source regions of the tephra found in the ash layers, the abundances of major and, in one case, trace elements for the tephra particles were measured by means of electron-probe microanalyzer (EPMA) and laser-ablation inductively coupled plasma mass spectrometer (LA-ICP-MS), respectively.

The chemical and isotopic composition of volcanic ash found in an ice core from Vostok was reported in Basile and others (2001). They determined the origin of fourteen ash layers as follows: nine from the South Sandwich Islands, Southern Ocean, three from southern South America, one from the Antarctic Peninsula and one from Marie Byrd Land, Antarctica. In order to correlate between the Dome Fuji and Vostok cores, Fujii and others (1999) compared the positions of all of the respective tephra layers on profiles of isotopic ratios: $\delta^{18}O$ of the Dome Fuji core and δD of the Vostok core (Fig. 2), which are linearly related with a slope close to eight (Vimeux and others, 2002). They found that eight layers were correlated as the following depths of Dome Fuji and Vostok ash layers, respectively: 505–369 m, 1128 or 1129 m to 988 m, 1361–1280 m, 1568–1508 m, 1849 or 1852 m to 1991 or 1995 m, 2026–2325 m, 2117–2501 m and 2170–2586 m. Hence, we have verified that tephra layers are coeval based on the chemical abundances of their tephras found in the two cores.

SAMPLES

The 26 ash layers found in the Dome Fuji core have distinct boundaries and are light gray to yellow in color (Fujii and

https://doi.org/10.3189/172756404781813934 Published online by Cambridge University Press

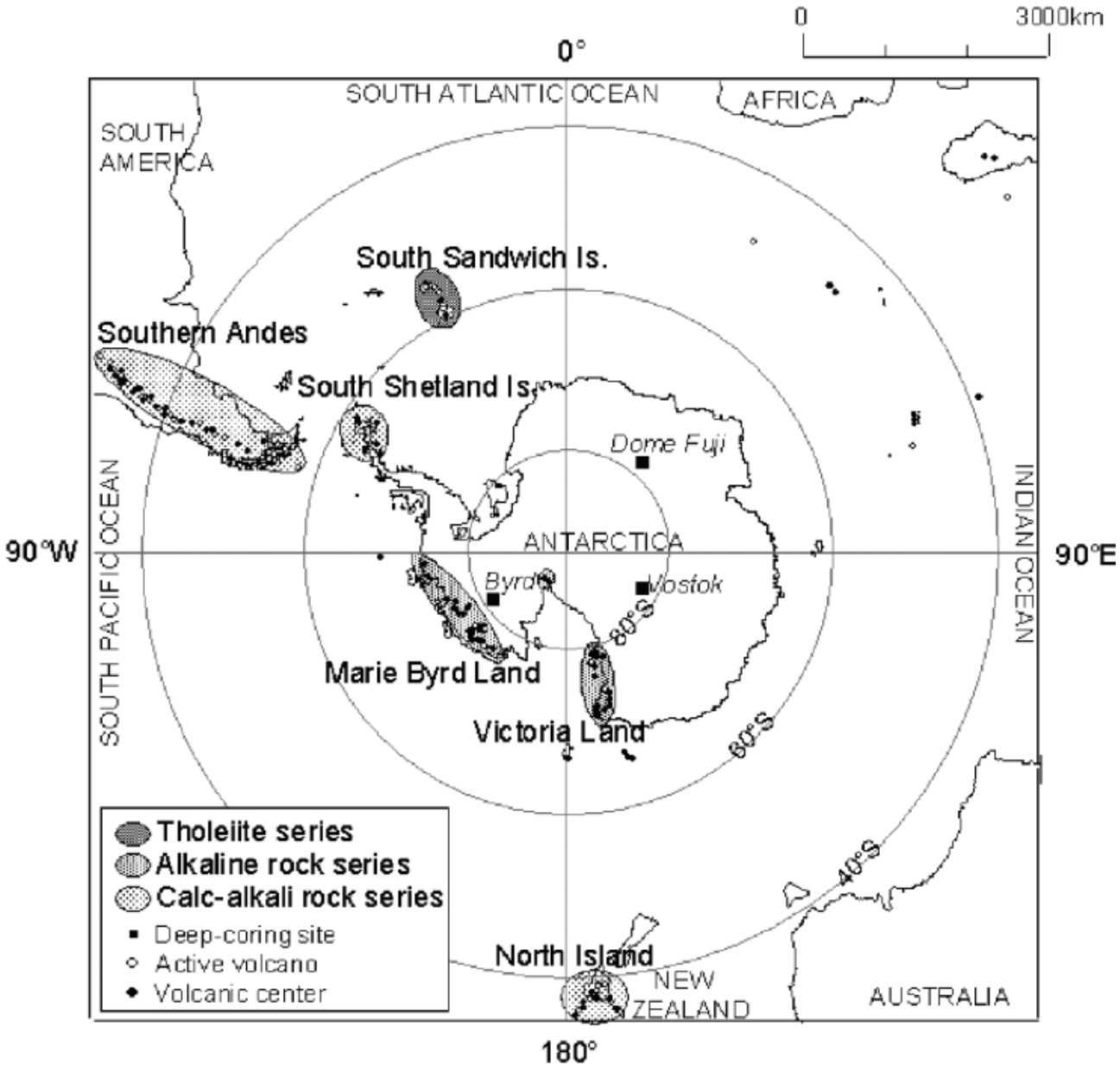

Fig. 1. Location of Dome Fuji and other deep ice-coring sites in Antarctica. The late Cenozoic volcanoes and active volcanoes are indicated by solid and open circles, respectively. Shaded areas are labeled by dominant rock series.

others, 1999; Table 1). The ages of the ice containing the ash layers were determined based on the relation between the annual-layer thickness and $\delta^{18}O$ values, combined with a simple steady-state ice-flow model (Dansgaard and Johnsen, 1969) by Watanabe and others (2003). The tephra-containing layers were 1–24 mm thick, suggesting that the duration of ash fallout ranges from a few months to 5 years on the basis of the preceding model. The long duration of the tephra fallout implies that the fine tephras were intermittently ejected from the source to the upper troposphere and/or stratosphere and suspended there for long periods.

ANALYTICAL PROCEDURE

Sample preparation

A small piece of ice (10–100 mg) was collected from the ash layer with a small stainless-steel chisel. The ice was placed on a thin quartz-glass on a hot plate and evaporated to dryness at 50°C. All these procedures were carried out in a clean bench in a low-temperature room at –20°C.

The ash on the glass was covered with a drop of Petropoxy Resin #154 (Palouse Petro Products), which was then allowed to solidify on the hot plate at a temperature of ~150°C for 3 hours in a clean bench in a class 10 000 clean room. The resin containing the ash was polished until the tephra section was exposed.

The surface of the resin section was coated with carbon to make it conducting. Grain texture and size were investigated using a scanning electron microprobe (SEM; JSM-5200, JEOL) in order to determine analytical points in the tephra grains.

Major-elements analysis

Analysis of major-element oxides (SiO_2, TiO_2, Al_2O_3, FeO, MnO, MgO, CaO, Na_2O and K_2O) in glassy parts of the tephra samples was carried out using a wavelength-

https://doi.org/10.3189/172756404781813934 Published online by Cambridge University Press

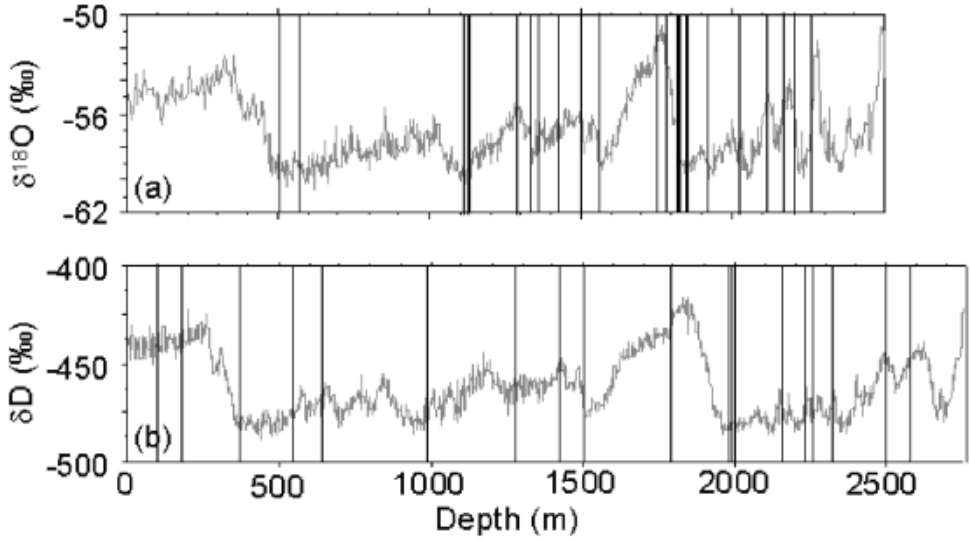

Fig. 2. Correlation of tephra layers found in both Dome Fuji (a) and Vostok (b) ice cores, based on $\delta^{18}O$ and δD profiles, respectively (Fujii and others, 1999).

dispersive EPMA (JXA-8800, Japanese Electron Optics Limited) equipped with five detectors at the National Institute of Polar Research, Tokyo, Japan, using the ZAF correction method (Duncumb and Reed, 1968). The glass was analyzed with an accelerating voltage of 15 keV and an electron-beam current of 12 nA. The electron-beam diameter was set at >5 μm in order to minimize migration of sodium and potassium during the analyses of aphyric groundmass. Devitrified tephra was, however, analyzed with a broader electron beam (10–20 μm), in order to obtain a mean chemical composition of groundmass without microphenocrysts. The intensity of sodium Kα X-rays decreased by about 25% during the first 10 s when the beam diameter was set at 5 μm. Therefore, counting time for sodium was reduced by 2 s in order to minimize loss of the sodium Kα X-ray. To obtain the mean composition of a single tephra particle, one to three points were analyzed.

Uncertainties of the measurements were tested by duplicate analysis of reference glasses under the same analytical conditions, but only for a beam diameter of 5 μm. The reference glasses were made of powder samples of natural igneous rock whose compositions had been precisely determined (Imai and others, 1995). Rock types of the powder samples 'Igneous rock series' provided by the Geological Survey of Japan were alkaline basalt (JB-1), high-alumina basalt (JB-3), dacite (JA-1), andesite (JA-3) and rhyolite (JR-1). Table 2 summarizes the reliability and precision (1 standard deviation (1σ)) of our electron microprobe analyses and recommended values of the powder rock samples (Imai and others, 1995). Differences in resulting abundance data between reported data and present data were within ±5% for JB-1 and JB-3, ±9% for JA-1 and JA-3, and ±10% for JR-1, except for Na_2O of JR-1 (–14%).

Table 1. Ash layers found in Dome Fuji ice core

Depth	Age	Thickness	Max. grain-size
m	kyr BP	mm	μm
505.80	19	2	30
573.87	24	8	50
1113.53	68	2	<10
1128.48	70	12	<10
1129.46	70	21	30
1295.22	85	3	30
1336.45	89	4	20
1361.89	92	8	30
1426.45	97	6	30
1499.84	104	3	<10
1568.41	113	4	<10
1759.12	131	4	30
1778.88	132	4	30
1785.14	132	13	30
1818.51	135	11	20
1820.92	135	9	30
1826.49	136	10	20
1849.55	141	24	30
1852.26	141	5	<10
1923.31	155	5	20
2008.12	173	5	20
2026.34	177	1	40
2117.75	204	2	40
2170.18	215	2	30
2202.81	213	8	40
2263.12	226	3	40

Trace-elements analysis

Abundances of 14 trace elements (rare-earth elements (REEs): La, Ce, Pr, Nd, Sm, Eu, Gd, Tb, Dy, Ho, Er, Tm, Yb and Lu) were measured by an ICP-MS (VG PlasmaQuad 2 Omega, ThermoElectron) equipped with an ArF Excimer laser ablation system (GeoLAS 200CQ, MicroLas) at Tokyo Institute of Technology. The advantages of using the laser ICP-MS system, compared with a solution nebulization system, are that (1) it can analyze solid tephra samples without prior digestion, (2) it requires a smaller amount of sample and (3) it can analyze a single tephra particle.

Helium gas, instead of Ar, was flushed into the sample cell in order to increase sample transport efficiency and reduce deposition of sample around the ablation pit (Eggins and others, 1998). Instrumental sensitivities thus achieved were >2000 Hz μg g^{-1} for Pb and U on NIST glass standard reference material 610 (NIST SRM 610 provided by US

https://doi.org/10.3189/172756404781813934 Published online by Cambridge University Press

Table 2. Test analyses of major element abundances (wt.%) of reference glasses[a] using EPMA

		Oxide										
		SiO_2	TiO_2	Al_2O_3	FeO*f	MnO	MgO	CaO	Na_2O	K_2O	Total	ng
JB-1a	Mean[b]	54.01	1.31	14.58	7.85	0.15	8.01	9.7	2.96	1.44	100	7
	1ρ[c]	0.41	0.05	0.26	0.06	0.01	0.06	0.11	0.07	0.03		
	Recom.[d]	53.68	1.31	14.8	8.27	0.15	8.02	9.54	2.8	1.43	100	
	Reliability[e] (%)	0.6	0.0	–1.5	–5.1	0.0	–0.1	1.7	5.7	0.7		
JB-3	Mean	51.8	1.44	17.09	10.28	0.18	5.4	10.23	2.81	0.78	100	7
	1ρ	0.27	0.03	0.04	0.13	0.02	0.19	0.05	0.1	0.02		
	Recom.	51.47	1.45	17.37	10.84	0.18	5.24	9.89	2.76	0.79	100	
	Reliability[e]	0.6	–0.7	–1.6	–5.2	0.0	3.1	3.4	1.8	–1.3		
JA-1	Mean	65.63	0.82	14.97	5.83	0.17	1.68	6.08	4	0.82	100	6
	1ρ	0.34	0.03	0.36	0.18	0.03	0.08	0.1	0.15	0.03		
	Recom.	65.02	0.86	15.47	6.41	0.16	1.6	5.79	3.9	0.78	100	
	Reliability[e] (%)	0.9	–4.7	–3.2	–9.0	6.3	5.0	5.0	2.6	5.1		
JA-2	Mean	58.49	0.66	15.94	5.44	0.12	7.42	6.64	3.44	1.86	100	9
	1ρ	0.2	0.03	0.41	0.04	0.01	0.12	0.07	0.21	0.07		
	Recom.	58.14	0.68	15.88	5.81	0.11	7.83	6.48	3.2	1.87	100	
	Reliability[e] (%)	0.6	–2.9	0.4	–6.4	9.1	–5.2	2.5	7.5	–0.5		
JR-1	Mean	77.41	0.1	12.9	0.81	0.11	0.11	0.76	3.51	4.29	100	14
	1ρ	0.44	0.04	0.08	0.03	0.02	0.02	0.02	0.12	0.11		
	Recom.	76.59	0.11	13.02	0.82	0.1	0.12	0.68	4.08	4.48	100	
	Reliability[e] (%)	1.1	–9.1	–0.9	–1.2	10.0	–8.3	11.8	–14.0	–4.2		

[a]Reference glasses made of reference powder samples 'Igneous rock series' distributed by Geological Survey of Japan (Imai and others, 1995). JB-1a, alkali basalt; JB-3, high-alumina basalt; JA-1, dacite; JA-3, andesite; JR-1, rhyolite.
[b]Mean values of analyses normalized by 100%.
[c]One standard deviation (1σ) of analyses.
[d]Recommended value (Imai and others, 1995) normalized to 100%.
[e]Reliability = $(V_{mean}/V_{recom.} - 1) \times 100$
[f]All iron calculated as FeO.
[g]Number of analyses.

National Institute of Standards Technology) from a pit diameter of 16 μm ablated at 5 Hz repetition rate with an output pulse energy of 140 mJ (Hirata, 2003). The spatial resolution (6.4 μm) achieved by the current LA-ICP-MS system was high enough to measure 14 trace elements in a single tephra grain. For precise and reliable abundance data, however, it was important to prepare homogeneous and matrix-matched standard reference materials. In this study, the NIST SRM 610 was used as a calibration standard, because the homogeneity of the NIST SRM 610 was well established through rigorous testing by many research groups over an extended period (Pearce and others, 1996). The matrix of the NIST SRM 610 is 72% SiO_2, 12% CaO, 14% Na_2O and 2% Al_2O_3.

The reliability and precision of our LA-ICP-MS analyses were tested by analyzing the trace-element abundances in NIST SRM 612 (similar in major composition to the SRM 610; abundances of trace elements are almost one-tenth the level of the NIST SRM 610). The abundance values for trace elements reported by Pearce and others (1996) are also summarized in Table 3. Differences in resultant abundance data between reported data and data of the present study were within ±10%, except for Lu (±17%). This level of precision of the measurement is enough to distinguish the difference in chemical composition of trace elements in tephras having different sources.

Resultant REE abundances were normalized to those of chondrites having the composition of the Earth's primitive mantle. Thereby, the fractionation of REE abundances through various geochemical processes can be recognized, because the terrestrial REE abundances are characterized as follows: elements having even atomic numbers are more abundant than their immediate neighbors with odd atomic numbers (e.g. Anders and Ebihara, 1982).

RESULTS AND DISCUSSION

Particle size and texture

Particles found in the ash layers were mainly groundmass glass fragments (glass shards), having angular edges and showing curved and smooth surfaces. Maximum sizes of tephras were < 50 μm as determined by SEM observation. Particles found in five layers at depths of 1113, 1128, 1499, 1568 and 1852 m were < 5 μm.

SEM observation revealed that the tephras found in layers at 573, 1426 and 1826 m were strongly devitrified and poorly vesiculated. They are mostly composed of euhedral microphenocrysts and euhedral to subhedral microlites with a minor quantity of interstitial glasses. Part of the microlites and the glasses in them were analyzed with a broad beam at 10–20 μm. Vitreous tephras were found at depths of 1336, 1361, 1785, 1818, 2008, 2202 and 2263 m. They were moderately vesiculated and some of them showed well-developed elongate vesicles. The tephras found in the other layers were composed of both devitrified and vitreous matrix glasses. These vitreous tephras were analyzed with a beam at 5 μm.

Tephras found in the 21 layers with particle sizes of a few tens of μm, except for the five layers at depths of 1113, 1128, 1499, 1568 and 1852 m, were derived from source

https://doi.org/10.3189/172756404781813934 Published online by Cambridge University Press

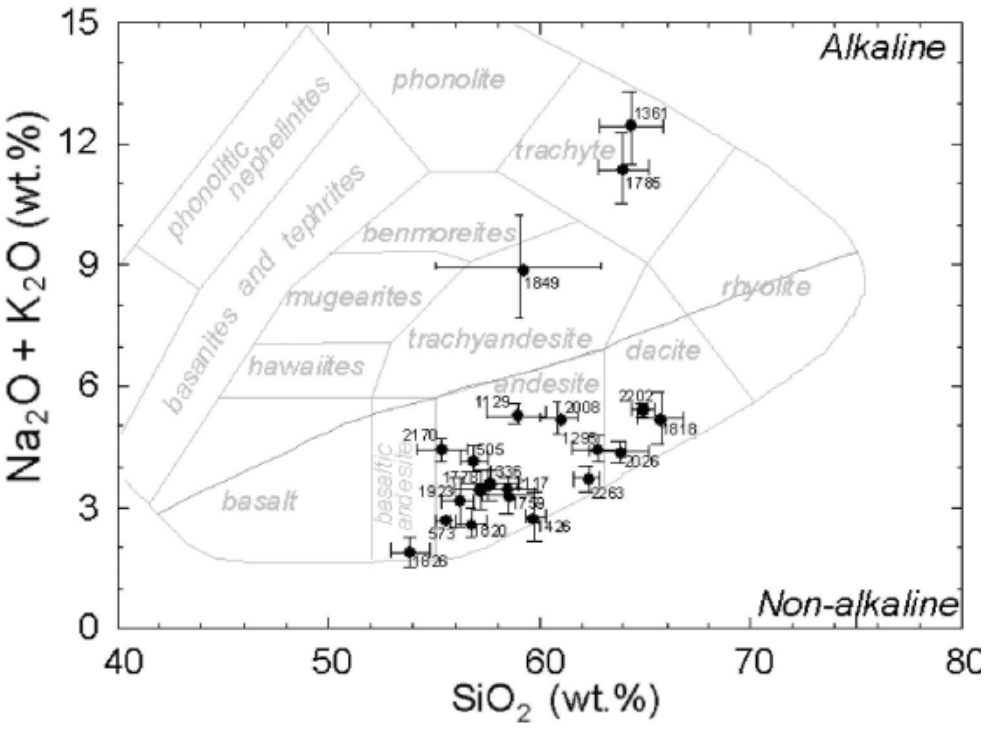

Fig. 3. Diagram of SiO_2 vs total alkalis (Na_2O+K_2O) for analyzed tephras found in the Dome Fuji ice core. Error bars show one standard deviation (1σ) corresponding to variation of analyzed tephra samples. Dashed line indicates a boundary between alkaline and non-alkaline rock fields (Miyashiro, 1978). Nomenclature is cited from Cox and others (1979).

volcanoes not very far from Dome Fuji, probably in the Antarctic region (Fig. 1). In sharp contrast, the tephra particles with sizes of <5 μm collected from those five layers were likely transported over longer distances, from volcanoes located in more distant regions of the lower latitudes (e.g. Cole-Dai and others, 1997).

Table 3. Test analyses of trace-element abundances (ppm) of a reference glass using LA-ICPMS

Element	NIST SRM 612[a]				Reliability[e]	%SD[f]
	Mean[b]	1σ[c]	Recom.[d]	1σ	%	
La	39	0.1	35.77	2.15	8.2	0.1
Ce	39	1.6	38.35	1.64	1.4	4.2
Pr	39	2.6	37.16	0.93	4.8	6.6
Nd	37	3.4	35.24	2.44	3.9	9.4
Sm	35	2.9	36.72	2.63	–4.1	8.3
Eu	36	2.1	34.44	1.59	5.8	5.8
Gd	41	3.5	36.95	1.06	10.8	8.6
Tb	39	2.4	35.92	2.68	9.1	6.1
Dy	38	3.8	35.97	0.82	6.9	9.8
Ho	40	2.7	37.87	1.09	4.4	6.9
Er	41	3.0	37.43	1.50	9.9	7.2
Tm	40	2.6	37.55	1.25	5.3	6.6
Yb	40	3.6	39.95	2.86	–0.4	9.0
Lu	44	3.4	37.71	1.95	16.9	7.7
n[g]	12					

[a]The silica glass reference material was Standard Reference Material (SRM) 612, produced by the US National Institute of Standards and Technology (Pearce and others, 1996).
[b]Mean value of analyses.
[c]One standard deviation (1σ) of analyses.
[d]Recommended value (Pearce and others, 1996).
[e]Reliability = $(V_{mean}/V_{recom.}-1)\times 100$.
[f]%SD = $(1\sigma_{mean}/V_{mean})\times 100$.
[g]Number of analyses.

Major-element composition

Volcanic rocks are generally classified into two types based on the relation between total alkalis (Na_2O+K_2O) and silica (SiO_2) contents, namely, the alkaline and non-alkaline rock series. The contents of total alkali and silica have been widely used for the chemical classification of igneous rocks (Cox and others, 1979; Fig. 3). The non-alkaline rock series are further classified into two types of rock series based on the proportion of total iron ($FeO+Fe_2O_3$), Na_2O+K_2O and MgO, namely, the calc-alkaline and tholeiitic rock series. Volcanic rocks obtained from the volcanoes in the Antarctic are classified into these three rock series as shown in Figure 1.

Major-element compositions of the tephras in the 21 layers, except for the 5 layers at depths of 1113, 1128, 1499, 1568 and 1852 m, were determined by the EPMA. The tephras from these 5 layers were smaller than 5 μm, so they could not be polished. The number of analyzed particles ranged from 5 to 27 for each sample. The resultant Na_2O+K_2O concentrations are plotted against SiO_2 concentrations in Figure 3. These tephras were classified into the alkaline (trachyandesite to trachyte) and the non-alkaline (basaltic andesite to dacite) rock series. The tephras found at depths of 1361, 1785 and 1849 m corresponded to trachyandesite and trachyte, indicating that their source regions are Marie Byrd Land and/or Victoria Land, Antarctica (Fig. 1). The non-alkaline tephras were further classified into two groups, tholeiite and calc-alkaline rock series based on the proportion of $FeO+Fe_2O_3$, Na_2O+K_2O and MgO (Fig. 4). The tephras, except for 1129, 2008 and 2170 m tephras, plot within the tholeiite rock field (Naraoka and others, 1991), suggesting that most of the tephras found

https://doi.org/10.3189/172756404781813934 Published online by Cambridge University Press

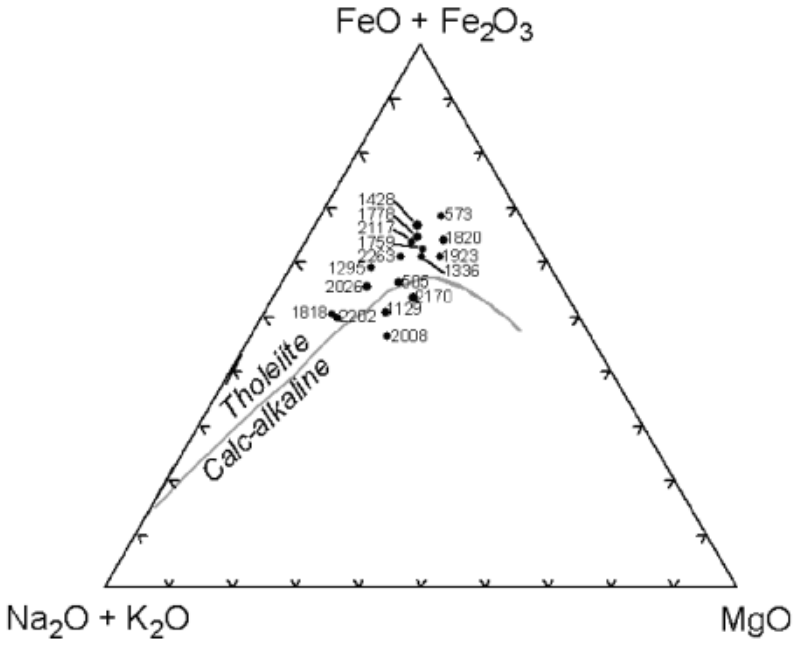

Fig. 4. Diagram of total alkalis ($Na_2O + K_2O$)–total iron–MgO for analyzed tephras in the Dome Fuji ice core. Dashed line indicates a boundary between tholeiite and calc-alkaline rock series (e.g. Kuno, 1950).

in the Dome Fuji core originate from the South Sandwich Islands. The other tephras from the three layers at 1129, 2008 and 2170 m were classified as calc-alkaline basaltic andesite to andesite (Figs 3 and 4). Three source candidates for the volcanic regions which produced the calc-alkaline rock are shown in Figure 1: the South Shetland Islands, the southern part of the Andes, and the North Island of New Zealand. The tephras from the North Island of New Zealand, however, are much more silicic than those from the three layers, making it more likely that the tephras were transported from the South Shetland Islands and/or the southern part of the Andes.

The magnitude of 1σ for SiO_2 and $Na_2O + K_2O$ concentrations of the 1849 m tephra was much higher than that of the other tephras (Fig. 3). Representative variation diagrams of SiO_2 vs $Na_2O + K_2O$, K_2O, FeO and TiO_2 for all analyzed tephras from the layer are shown in Figure 5. The data points define a single straight line, probably resulting from compositionally zoned magma following fractional crystallization (e.g. Mandeville and others, 1996).

Trace-element composition

REE abundances were measured to obtain geochemical and petrogenetic information. A chemical property of the trivalent REEs is that their ionic radii systematically vary with atomic numbers, whereas the electronic configurations of their outer electron orbits remain the same. Therefore, the REEs are identical, except for their ionic radii, with regard to partitioning between mineral and melt in magmas. Due to systematic differences in ionic radii (McKay, 1989), the relative REE abundances would change sensitively through metamorphic events or mineralization processes, and the REE abundance data can be used for identification of source volcanoes (Fukuoka and others, 1987).

For the 1361 m tephra, which is considered to originate from Marie Byrd Land or Victoria Land based on the major-element abundances, the REE abundances were measured using the LA-ICP-MS technique. Only three particles were analyzed because the LA-ICP-MS analysis required large (>20 μm) and homogeneous samples. The REE abundances of the tephra and the volcanic rocks from the two source regions are shown in Figure 6 (LeMasurier and others, 1976; Rocholl and others, 1995). The REE variation pattern of the tephra plots within that of Marie Byrd Land, indicating that the 1361 m tephra originated from a volcano in Marie Byrd Land.

Comparison with Vostok tephras

We compared individual major-element abundances of the tephras found in the eight coeval tephra layers between the Dome Fuji and Vostok (Palais and others, 1989b; Basile and others, 2001) ice cores (Table 4). The major-element abundances of their tephras, except for the 1128, 1568 and 1852 m tephras which were not large enough to analyze, are listed in Table 4.

The tephra found in the 1361 m deep layer of the Dome Fuji core was classified into the alkaline rock series. Two types of tephra found in a 1280 m layer of the Vostok core were classified into the calc-alkaline and tholeiite rock series, indicating that the 1361 m layer of the Dome Fuji core was not coeval with the 1280 m layer of the Vostok core.

The tephra found in the 1849 m layer in the Dome Fuji core corresponds to trachyandesite. The tephra found in the 1991 m deep layer of the Vostok core corresponds to basaltic andesite, suggesting that these two layers are not coeval.

We calculated the 'similarity coefficients' proposed by Borchardt and others (1972), commonly used for correlating tephras (e.g. Fiacco and others, 1993). This coefficient is expressed as a function of ratios between abundances of each element and relative dispersions. The coefficient is defined as 1 for perfectly identical tephras, and 'similar' tephras have >0.85 (Zielinski and others, 1995). The similarity coefficient of the compositions of the tephras at depths of 505–369 m, 1129–988 m, 2026–2325 m, 2117–2501 m and 2170–2586 m ranged from 0.85 to 0.95, except

https://doi.org/10.3189/172756404781813934 Published online by Cambridge University Press

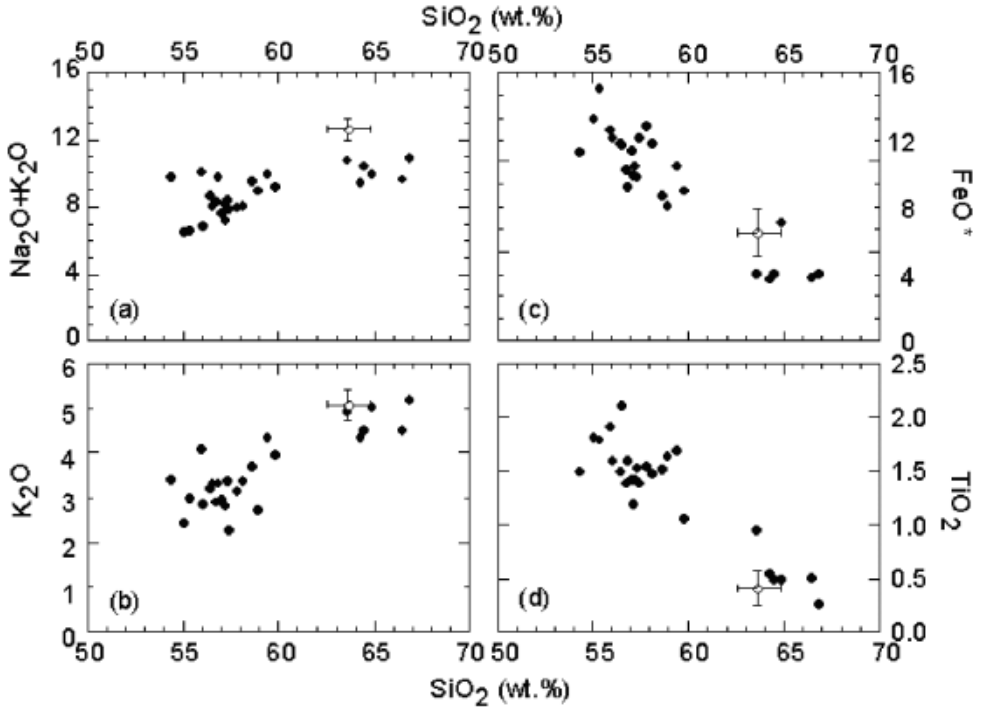

Fig. 5. Variation diagrams of SiO_2 vs (a) total alkalis ($Na_2O + K_2O$), (b) K_2O, (c) FeO and (d) TiO_2. Solid and open circles indicate the 1849 m and 1995 m tephras found in Dome Fuji and Vostok ice cores, respectively. The abundances of the 1995 m tephra are a mean value (Basile and others, 2001), and the error bars are the same as in Figure 2.

for the tephras at depths of 1361–1280 m and 1849 m to 1991 or 1995 m.

The tephras found in the 1849 m layer of the Dome Fuji core and the 1996 m layer of the Vostok core were classified into the alkaline rock series (Fig. 2; Table 4), although the similarity coefficient (0.73) was much lower than 0.85. Thicknesses of these layers at 1849 m and 1996 m are relatively great (24 and 20 mm, respectively). Figure 4 shows that the 1996 m tephra of the Vostok core plots close to the trend of the 1849 m tephra of the Dome Fuji core. This indicates that the 1849 m and 1996 m tephras found in the Dome Fuji and Vostok cores, respectively, may be identical, whereas trachyandesitic tephras have not yet been found in the Vostok core.

Consequently, six tephra layers are common to the Dome Fuji and Vostok cores (505–369 m, 1129–988 m, 1849–1995 m, 2026–2325 m, 2117–2501 m and 2170–2586 m). Each of these tephras may have covered most of the surface of the Antarctic ice sheet at one time. Therefore, these layers have a high potential for being the key correlation beds among deep ice cores from Antarctica.

CONCLUSIONS

Major-element abundances of tephras from 21 tephra layers found in the Dome Fuji core were measured using EPMA. In addition, REE abundance of one of these (1361 m) was measured using LA-ICP-MS. We hope that this method,

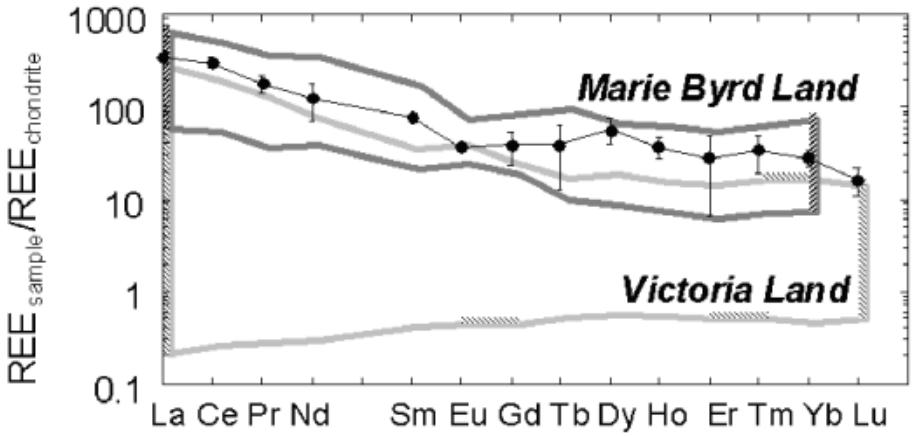

Fig. 6. Variation pattern of REEs of the 1361 m tephra. Fields enclosed by heavy and light broken lines indicate variation ranges of tephras from volcanoes in Marie Byrd Land and Victoria Land, respectively (LeMasurier and others, 1976; Rocholl and others, 1995). Error bars are the same as in Figure 2.

https://doi.org/10.3189/172756404781813934 Published online by Cambridge University Press

Table 4. Major-element analyses of glass shards (wt.%) obtained from common layers between the Dome Fuji and Vostok ice cores

		Oxide											
		SiO_2	TiO_2	Al_2O_3	FeO*[d]	MnO	MgO	CaO	Na_2O	K_2O	Total	n[e]	Ref.[f]
505 m	Mean[b]	56.79	1.96	15.64	9.34	0.16	3.54	7.02	3.44	0.76	98.67	10	
	1ρ[c]	0.68	0.17	0.53	1.13	0.05	0.22	0.40	0.35	0.08			
V369 m[a]		57.62	1.02	15.38	11.00	0.24	2.89	7.44	3.51	0.40	99.50	25	1
		1.85	0.21	2.07	2.46	0.13	1.38	0.72	0.70	0.11			
1129 m		58.75	2.15	15.76	8.90	0.18	2.70	5.87	4.40	0.93	99.63	8	
		1.43	0.32	0.52	0.48	0.03	0.21	0.23	0.29	0.12			
V988 m		55.50	2.45	17.08	8.09	0.15	3.13	7.49	4.78	0.67	99.34	31	2
		1.93	1.17	2.02	1.74	0.10	0.86	1.25	0.62	0.26			
1361 m		64.02	0.54	14.38	8.34	0.29	0.04	1.27	8.01	4.38	101.27	16	
		1.51	0.04	0.49	0.45	0.05	0.03	0.25	0.77	0.29			
V1280 m	Type a	64.62	0.78	14.74	8.55	0.20	1.95	6.29	2.20	0.47	99.80	14	2
		1.15	0.12	0.69	0.99	0.09	0.25	0.38	0.45	0.07			
V1280 m	Type b	66.62	0.59	14.71	9.11	0.34	0.08	1.50	2.34	4.46	99.75	33	2
		0.96	0.08	0.64	0.44	0.09	0.05	0.35	0.27	0.24			
1849 m		58.90	1.32	16.11	9.18	0.24	1.25	4.11	5.26	3.58	99.95	28	
		3.71	0.49	0.81	2.46	0.06	0.58	1.36	0.75	0.82			
V1995 m		63.68	0.41	14.40	6.85	0.45	0.03	1.08	7.55	5.08	99.53	17	2
		1.15	0.16	1.04	1.03	0.45	0.04	0.32	0.56	0.34			
2026 m		63.67	0.84	14.11	8.01	0.23	1.61	5.65	3.98	0.40	98.48	10	
		1.40	0.06	0.17	0.46	0.06	0.08	0.20	0.29	0.04			
V2325 m		65.59	0.91	14.30	8.67	0.23	1.65	5.93	1.88	0.47	99.63	10	2
		0.46	0.07	0.22	0.32	0.06	0.13	0.15	0.15	0.04			
2117 m		58.66	1.17	15.15	10.09	0.28	2.60	6.88	3.35	0.44	98.62	8	
		1.33	0.15	0.93	1.53	0.06	0.56	0.49	0.54	0.06			
V2501 m		62.59	0.74	15.40	8.07	0.19	1.90	6.29	3.93	0.48	99.59	16	2
		0.71	0.30	0.90	0.83	0.06	0.36	0.45	0.32	0.08			
2170 m		55.41	1.38	15.72	9.42	0.17	3.64	7.74	3.45	0.90	97.84	10	
		1.38	0.08	0.44	0.66	0.04	0.53	0.69	0.26	0.14			
V2586 m		56.53	1.46	16.39	8.90	0.19	3.49	7.66	3.82	0.98	99.42	14	2
		0.81	0.47	1.14	1.67	0.08	0.40	0.44	0.49	0.22			

[a]Depth of an ash layer found in the Vostok ice cores.
[b]Mean values of analyses.
[c]One standard deviation (1σ) of analyses.
[d]All iron calculated as FeO.
[e]Number of analyses.
[f]Sources: 1. Palais and others (1989b); 2. Basile and others (2001).

which requires only small amounts of sample, will be a useful tool for correlating tephras preserved in ice cores.

Six ash layers were found to be common to the Dome Fuji and Vostok ice cores, on the basis of their abundances of major and trace elements. This indicates the possibility for correlating these particular tephras with those present in other Antarctic ice cores, and possibly in sea sediment cores around Antarctica.

ACKNOWLEDGEMENTS

We thank T. Iizuka and T. Ohno of the Tokyo Institute of Technology for supporting the LA-ICP-MS analyses, and dust research members of the Dome Fuji project for their help with observing tephra layers. We also acknowledge T. K. Hinkley of the US Geological Survey, and two reviewers, C. U. Hammer of the University of Copenhagen and J. M. Palais of the US National Science Foundation, for valuable comments.

REFERENCES

Anders, E. and M. Ebihara. 1982. Solar-system abundances of the elements. *Geochim. Cosmochim. Acta,* **46**(11), 2363–2380.

Basile, I., J.-R. Petit, S. Touron, F. E. Grousset and N. I. Barkov. 2001. Volcanic tephra in Antarctic (Vostok) ice-cores: source identification and atmospheric implications. *J. Geophys. Res.,* **106**(D23), 31,915–31,931.

Borchardt, G. A., P. J. Aruscavage and H. T. Hamilton, Jr. 1972. Correlation of the Bishop ash, a Pleistocene marker bed, using instrumental neutron activation analysis. *J. Sediment. Petrol.,* **42**(2), 301–306.

Cole-Dai, J., E. Mosley-Thompson and L. G. Thompson. 1997. Quantifying the Pinatubo volcanic signal in south polar snow. *Geophys. Res. Lett.,* **24**(21), 2679–2682.

Cox, K. G., J. D. Bell and R. J. Pankhurst. 1979. *The interpretation of igneous rocks.* London, George Allen and Unwin.

Dansgaard, W. and S. J. Johnsen. 1969. A flow model and a time scale for the ice core from Camp Century, Greenland. *J. Glaciol.,* **8**(53), 215–223.

Dome-F Deep Coring Group. 1998. Deep ice-core drilling at Dome Fuji and glaciological studies in east Dronning Maud Land, Antarctica. *Ann. Glaciol.,* **27**, 333–337.

Duncumb, N. W. and J. B. Reed. 1968. *Quantitative electron probe microanalysis.* Washington, DC, US Department of Commerce. (National Bureau of Standards Special Publication 298.)

Eggins, S. M. L., P. J. Kinsley and J. M. G. Shelley. 1998. Deposition and elemental fractionation processes during atmospheric pressure laser sampling for analysis by ICP-MS. *Appl. Surf. Sci.,* **127**(12), 278–286.

https://doi.org/10.3189/172756404781813934 Published online by Cambridge University Press

Fiacco, J. R., Jr, J. M. Palais, M. S. Germani, G. A. Zielinski and P. A. Mayewski. 1993. Characteristics and possible source of 1479 A.D. volcanic ash layer in a Greenland ice core. *Quat. Res.,* **39**(3), 267–273.

Fujii, Y. *and 8 others*. 1999. Tephra layers in the Dome Fuji (Antarctica) deep ice core. *Ann. Glaciol.,* **29**, 126–130.

Fukuoka, T., F. Arai and F. Nishio. 1987. Correlation of tephra layers in Antarctic ice by trace element abundances and refractive indices. *Bull. Volcanol. Soc. Japan, Ser. 2,* **32**(2), 103–118.

Gow, A. J. and T. Williamson. 1971. Volcanic ash in the Antarctic ice sheet and its possible climatic implications. *Earth Planet. Sci. Lett.,* **13**(1), 210–218.

Hammer, C. U., H. B. Clausen and W. Dansgaard. 1980. Greenland ice sheet evidence of post-glacial volcanism and its climatic impact. *Nature,* **288**(5788), 230–235.

Hirata, T. 2003. Chemically assisted–laser ablation–inductively coupled plasma–mass spectrometry. *Anal. Chem.,* **75**(2), 228–233.

Imai, N., S. Terashima, S. Ito and A. Ando. 1995. 1994 compilation values for GSJ reference samples, 'igneous rock series'. *Geochemical Journal,* **29**(1), 91–95.

Kuno, H. 1950. Geology of Hakone volcano and adjacent area. Part 1. *Journal of Faculty of Science, Tokyo University. Section II 7*, 257–279.

Kyle, P. R. and P. A. Jezek. 1978. Compositions of three tephra layers from the Byrd Station ice core, Antarctica. *J. Volcanol. Geotherm. Res.,* **4**(4), 225–232.

Kyle, P. R., P. A. Jezek, E. Mosley-Thompson and L. G. Thompson. 1981. Tephra layers in the Byrd Station ice core, Antarctica, and their climatic importance. *J. Volcanol. Geotherm. Res.,* 11, Special issue: Volcanism and climate, 29–39.

Kyle, P. R., J. Palais and E. Thomas. 1984. The Vostok tephra: an important englacial stratigraphic marker? *Antarct. J. US,* **19**(5), 64–65.

LeMasurier, W. E., P. R. Kyle and P. C. Rankin. 1976. Rare-earth element geochemistry of volcanic rocks from the Executive Committee Range, Marie Byrd Land. *Antarct. J. US,* **11**(4), 263–267.

Mandeville, C., S. Carey and H. Sigurdsson. 1996. Magma mixing, fractional crystallization, and volatile degassing during the 1883 eruption of Krakatau volcano, Indonesia. *J. Volcanol. Geotherm. Res.*, **74**(3–4), 243–274.

McKay, G. A. 1989. Partitioning of rare earth elements between major silicate minerals and basaltic melts. *Reviews in Mineralogy,* **21**, 45–78.

Miyashiro, A. 1978. Nature of alkalic volcanic rock series. *Contrib. Mineral. Petrol.,* **66**, 91–104.

Naraoka, H., K. Yanai and S. Fujita. 1991. [Dirt bands in the bare ice area around Sør Rondane Mountains in Queen Maud Land, Antarctica.] *Antarct. Rec.,* **35**, 47–55. [In Japanese.]

Palais, J. M. 1985. Particle morphology, composition and associated ice chemistry of tephra layers in the Byrd ice core: evidence for hydrovolcanic eruptions. *Ann. Glaciol.*, **7**, 42–48.

Palais, J. M., E. Mosley-Thompson and E. Thomas. 1987. Correlation of a 3,200 year old tephra in ice cores from Vostok and South Pole stations, Antarctica. *Geophys. Res. Lett.,* **14**(8), 804–807.

Palais, J. M., S. Kirchner and R. Delmas. 1989a. Identification and correlation of volcanic eruption horizons in a 1,000-year ice-core record from the South Pole. *Antarct. J. US,* **24**(5), 101–104.

Palais, J. M., J.-R. Petit, C. Lorius and Ye. S. Korotkevich. 1989b. Tephra layers in the Vostok ice core: 160,000 years of Southern Hemisphere volcanism. *Antarct. J. US,* **24**(5), 98–100.

Palais, J. M., S. Kirchner and R. J. Delmas. 1990. Identification of some global volcanic horizons by major element analysis of fine ash in Antarctic ice. *Ann. Glaciol.,* **14**, 216–220.

Pearce, N. J. G. *and 6 others*. 1996. A compilation of new and published major trace element data for NIST SRM 610 and NIST SRM 612 glass reference materials. *Geostandards Newsl.,* **21**(1), 115–144.

Rocholl, A., M. Stein, M. Molzahn, S. R. Hart and G. Wörner. 1995. Geochemical evolution of rift magmas by progressive trapping of a stratified mantle source beneath the Ross Sea Rift, northern Victoria Land, Antarctica. *Earth Planet. Sci. Lett.,* **131**(3–4), 207–224.

Vimeux, F., K. M. Cuffey and J. Jouzel. 2002. New insights into Southern Hemisphere temperature changes from Vostok ice cores using deuterium excess correction. *Earth Planet. Sci. Lett.,* **203**(4), 829–843.

Watanabe, O. *and 6 others*. 2003. Dating of the Dome Fuji, Antarctica deep ice core. *Nat. Inst. Polar Res. Mem., Ser. Special Issue* 57, 25–37.

Zielinski, G. A. *and 6 others*. 1995. Evidence of the Eldgjá (Iceland) eruption in the GISP2 Greenland ice core: relationship to eruption processes and climatic conditions in the tenth century. *Holocene,* **5**(2), 129–140.

https://doi.org/10.3189/172756404781813934 Published online by Cambridge University Press